Desalination and Water Treatment
www.deswater.com

doi: 10.5004/dwt.2018.22994

133 (2018) 20–27
November

Thermodynamic and kinetics study of phosphonium-based cellulose acetate supported ionic liquid membrane: wastewater treatment

Sana Zulfiqar[a,*], Uzaira Rafique[a], M. Javed Akhtar[b], Azhar Hussain[c], Saira Mansab[a]

[a]*Department of Environmental Sciences, Fatima Jinnah Women University, Rawalpindi, Pakistan,*
emails: sanazulfiqar@fjwu.edu.pk (S. Zulfiqar), uzairaiqbal@yahoo.com (U. Rafique), saira.mansab90@gmail.com (S. Mansab)
[b]*Physics Division, Pakistan Institute of Nuclear Science & Technology, P.O. Nilore, Islamabad, Pakistan, email: javedakhtar6@gmail.com*
[c]*Department of Soil Science, University College of Agriculture & Environmental Sciences, TheIslamia University of Bahawalpur, Bahawalpur, 63100-Pakistan, email: azharhaseen@gmail.com*

Received 23 February 2018; Accepted 24 August 2018

ABSTRACT

The widespread use of pesticides and insecticides for agricultural and nonagricultural purposes have resulted in the presence of their residues in different environmental compartments and remain serious concern for polluting water bodies after industrial revolution, late 1960s. In this research work, carcinogenic insecticide "Pirimicarb" has been remediated from wastewater using an adsorption process. Phosphonium-based ionic liquid $[P(Cy)_3][BF_4^-]$ (PIL) and cellulose acetate supported IL membrane $([CA\text{-}P(Cy)_3][BF_4]^-)$(CA-PIL) were synthesized and characterized as adsorbents for Pirimicarb removal. Results of Fourier-transform infrared spectroscopy and scanning electron microscopy confirmed successful preparation of PIL and then incorporation in CA structure. Various parameters (concentration, temperature, and adsorbent mass) were analyzed using ultra violet-visible spectroscopy under close batch mode of 200 min. Comparison of percentage removal between PIL and CA-PIL membrane revealed better adsorption trend by CA-PIL membrane (72%) as compared with the prepared PIL (55%). Thermodynamic studies by calculating ΔG, ΔH, and ΔS showed that the reaction is an endothermic physiochemical sorption process. Kinetic studies favored pseudo-second-order Langmuir, Freundlich, and Temkin isotherms.

Keywords: Ionic liquid; Membrane; Phosphonium; Pirimicarb; Cellulose acetate; Orchard wastewater

1. Introduction

Water pollution due to extensive use of insecticides and pesticides is a major environmental concern. Rachel Carson (1962) in her book "Silent Spring" has raised the issue of pesticide use and its environmental impacts after the Green Revolution. Pesticide residues are mostly leached from crops, fruits and primarily move from agricultural fields and orchards to surface water as direct run-off, careless disposal and equipment washing [1,2]. There is a wide range of insecticides including carbamates, organophosphorus, pyrethroids use for controlling pests on vegetable crops [3]. Pirimicarb is a carcinogen and a common substituent of the *N*-methyl carbamate class of insecticides. Due to the high toxicity profile of carbamate, especially Pirimicarb [4] and its long-term persistence in the environment [5], the Food and Agricultural Organization (FAO) and the World Health Organization (WHO) have recommended an acceptable daily intake of 0–0.02 mg/kg [6,7].

The design of chemicals and the use of structure–activity relationships are essential tools to deliver safer chemicals with enhanced technical performance [8,9]. To tackle the problems associated with these pollutants is to degrade or to adsorb them using membranes, gels or nanoparticles. Adsorption contributes positively toward remediation of the environment especially by removing different pollutants from soil, air, and water ecosystem.

---

* Corresponding author.

1944-3994/1944-3986 © 2018 Desalination Publications. All rights reserved.

Various adsorbents have been used to reduce water pollution by removing pesticides, that is, zeolites, carbon nanotubes, metal organic frameworks, and nanoparticles [10–13].

Ionic liquids (IL) have been used as solvent medium in different chemical reactions for environmental remediation but very few scientists [14,15] considered them so far. These liquids (IL) show unique, diverse, and tunable properties comparing with conventional molecular compounds and possess better ionic conductivity and very less volatility [16]. These are directly linked with green chemistry and clean technology field [17] due to their distinctive properties [18] and can be applied as adsorbents for the removal of persistent organic pollutants.

The room temperature ionic liquids have been synthesized by the addition of IL monomer to fill all the interstitial spaces of porous material [19]. This process was also followed by etching and cross linking treatment. Results showed that there was an increase in surface area (150–220 m^2/g). Similarly 1-vinyl-3-hexylimidazolium-based ionic liquid and vinyl-modified magnetic particles were prepared for extraction of organophosphorus pesticides from tea and other drinks. Results supported satisfactory recovery of adsorbent (81.4%–112.6%) with relative standard deviation of 4.5%–11.3% [14].

The research work focuses on synthesis of phosphonium-based ionic liquid (PIL) and its cellulose acetate supported membrane (CA-PIL membrane) to investigate adsorptive behavior of Pirimicarb from orchard wastewater District Jehlum, Punjab, Pakistan.

2. Methodology

All reagents used were of analytical grade and were purchased from Merck (Germany) and Sigma Alrich (UK).

Synthesis of phosphonium-based ionic liquid

For synthesis of ionic liquid (PIL), tricyclohexyl phosphine salt (5 mmol) was added with Boron tetrafluoride complex (5 mmol) and toluene (20 mL). The mixture was subjected to heating (50°C) with continuous reflux of 24 h. An oily yellow solid was formed, indicating a metathesis in reaction. The product was condensed in ice bath (2–3 h), followed by the addition of triethylamine (10 mL) under vigorous shaking for 4 h. Synthesized product was purified by washing with ethyl acetate four to five times. Washed material was subjected to drying in vacuum (60°C) for 12 h following the methodology from literature [20]. Resultant is formation of phosphonium-based ionic liquid ($[P(Cy)_3][BF_4]^-$). Sample was coded as PIL.

2.1. Synthesis of cellulose acetate supported ionic liquid membranes

Phase inversion process was used for fabrication. 0.5 g of CA was dissolved in 50 mL acetone by continuous stirring at room temperature. The CA solution was kept under vacuum for a day so that homogenous viscosity is attained [21].

An aliquot of 10 mL of CA solution was added to prepare PIL followed by stirring for 30 min. Viscous syrup was fabricated onto glass slide and via phase inversion method in distilled water, the membrane was prepared (CA-$[P(Cy)_3][BF_4]^-$). This sample was coded as CA-PIL membrane. The BF_4 anion was chosen because of its hydrophilic character and the commercial availability of the corresponding chemical reactant for CA modification also reported by literature [22]. The fabrication results in intermolecular interactions between PIL and CA-PIL membrane due to the presence of acetyl and hydroxyl group present on surface of CA.

2.2. Batch adsorption experiments

The removal of Pirimicarb (adsorbate) using PIL and CA-PIL membrane was studied in close batch mode. Effect of various parameters, that is, time (200 min), concentration (3, 5, and 7 mg/L), and temperature (25°C, 35°C, 50°C, 70°C, and 100°C), was studied by keeping dose (10 mg) constant. Stock solution of adsorbate was prepared in 250 mL ethyl alcohol and aliquot of 30, 50, and 70 mL were taken separately in 100 mL volumetric flasks for studying the effect of varying parameters. All experiments were conducted in an applied chemistry laboratory and results were characterized using UV-vis spectrophotometer (UV-1601-Schimadzu, Japan). The percent removal of Pirimicarb from orchards wastewater has been studied using the following equation:

$$\%\,\text{Removal} = \frac{\left(C_i - C_t\right)}{C_i} \times 100 \tag{1}$$

2.3. Kinetic models and isotherms

Different kinetic models (first-order, pseudo-second order, and intraparticle diffusion [23]) and isotherms (Langmuir [24], Fruendlich [25], and Temkin [26]) were applied to prepare PIL and CA-PIL membrane in order to investigate the fitness of experimental data with the predicted one (Eqs. (1)–(6)). Linear equations used for kinetic models and isotherms [27] are as follows:

$$\log C_t = \left(\frac{K_1}{2.303}\right)t + \log C_o \tag{2}$$

Eq. (2) is first-order equation, where C_t is the concentration of adsorbate with respect to time, K_1 is first-order constant, t is the time, and C_o is initial concentration adsorbed at adsorbent surface.

$$\frac{t}{q_t} = \frac{1}{k^2 q_e^2} + \frac{t}{q_e} \tag{3}$$

Eq. (3) is for pseudo-second order, where q_t is the amount of adsorbate adsorbed with respect to time, q_e is the saturation of adsorbent active sites at equilibrium, and k^2 is pseudo-second order constant.

$$q_e = B\text{Ln}_t + B\text{Ln}C_e \tag{4}$$

Eq. (4) is Temkin equation, where $B = RT/b$, R = 8.314 J/mol K, T is the absolute temperature (K), b is the constant of heat sorption, t is the Temkin isotherm constant (L/g), and C_e

is the concentration of Pirimicarb adsorbed on adsorbent till equilibrium.

$$\frac{1}{q_e} = \frac{1}{q_t} + \frac{1}{b} q_o C_e \qquad (5)$$

Eq. (5) is Langmuir equation, where q_e is the amount adsorbed by adsorbent at equilibrium, q_t is the amount adsorbed with respect to time, b is the Langmuir constant, and q_o is the initial concentration.

$$\log q_e = \log k_f + \left(\frac{1}{n}\right) \log C_e \qquad (6)$$

where k_f is Freundlich constant (L/g) and n is the Freundlich exponent (g/L) in Eq. (6).

2.3.1. Intraparticular diffusion model

The rate controlling parameters describe mechanisms within intraparticle and membrane diffusion. According to Weber and Morris [28], an intraparticle diffusion coefficient K_{id} is given by the equation:

$$q_t = K_{\text{id}} \sqrt{t} + C \qquad (7)$$

where q_t is the amount of adsorbate adsorbed with time t, K_{id} is the intraparticular diffusion coefficient, t is the time, and C is the concentration of adsorbate used. The plot of q_t versus $t^{0.5}$ represents the initial curve and final linear portion that characterizes the two or more steps in the sorption process [29].

3. Characterization

Characterization techniques used were Fourier-transform infrared spectrophotometer (FTIR-8400 Shimadzu, Japan) and SEM for functional group identification and morphology prediction, respectively.

4. Results and discussion

FTIR spectroscopy

PIL are generally more stable [30,31] as compared with imidazolium based ILs. Fig. 1 shows the FTIR spectra of PIL and CA-PIL; the sharp peaks from 3,210 to 3,132 cm^{-1} in the spectra of PIL are attributed to CH stretching of benzene ring. Sharp peaks at 1,579 and 1,505 cm^{-1} are ascribed to C=C stretching of aromatic ring. Peak observed in the range of 1,385–1,263 cm^{-1} is assigned to CH in plane bending while out of plane bending peak at 901 and 836 cm^{-1} supported by researchers in literature [32]. Two sharp characteristic peaks at 1,106 and 1,041 cm^{-1} are due to BF stretching indicate successful binding of BF$_4$ cation with the cyclohexyl phosphonium. Furthermore, the comparison of FTIR spectrum of PIL with its CA membrane clearly shows the emergence of new broad band at 3,350 cm^{-1} that represents the presence of OH vibrations [33] of CA while OH bending can be observed at 1,414 cm^{-1}. The sharp peaks appeared at 3,120 and 2,980 cm^{-1} are of CH stretching of the benzene and the alkyl group, respectively. The peak at 1,650 cm^{-1} characterizes the presence of C=O stretching vibrations while the C–O peak of ester linkage of CA is observed at 1,240 cm^{-1}. Other peaks represent the PIL incorporation in CA membrane.

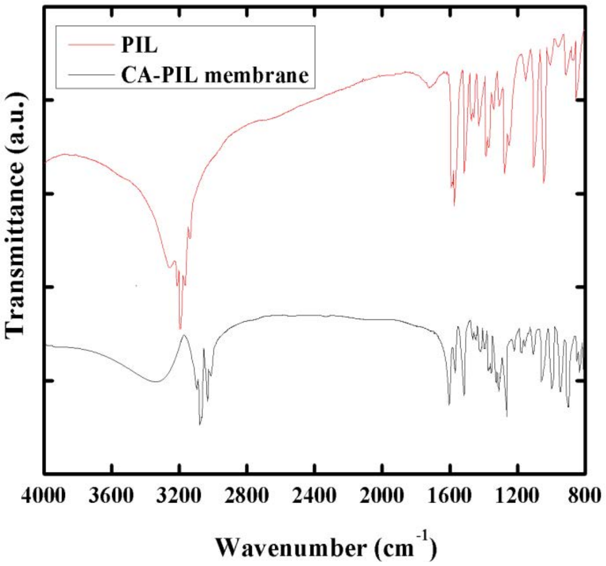

Fig. 1. FTIR overlay of PIL and CA-PIL membrane.

Scanning electron microscopy

Scanning electron microscopy (SEM) technique has been used to study the surface morphology of synthesized PIL and CA-PIL membrane. The SEM image of prestine CA membrane was taken from literature [34] (Fig. 2(a)), which showed a smooth dense surface before any organic/inorganic addition or incorporation. PIL shows fluffy loops like appearance [35] indicating successful synthesis [21] of hydrophobic PIL. Mostly cellulose-based films, gels, and membranes display uneven surface morphology [36]. Fabrication of synthesized PIL into membrane resulted into clear morphological change. The loop like structure of hydrophobic PIL was changed into thin fine water channels like appearance [37] after fabrication with CA (see Fig. 2(b)), confirming successful incorporation of PIL into CA matrix.

BET surface area analysis

Nitrogen sorption (adsorption–desorption) isotherm method has been employed to determine the pore volume. Sample was preheated under nitrogen gas flow for >2 h at 180°C to remove the moisture content before BET analysis. These results showed that synthesized PIL and CA-PIL membrane possesses 0.05 and 0.026 cm^3/g pore volume with BET surface area of 171 and 292 m^2/g, respectively, as shown in Table 1.

It can be depicted from the graph as shown in Fig. 3 that both synthesized adsorbents follows type IV sorption isotherm [38], which can be related to monolayer as well as multilayer sorption phenomenon with type 1 hysteresis loop [39] associated with mesoporous material having narrow size distribution.

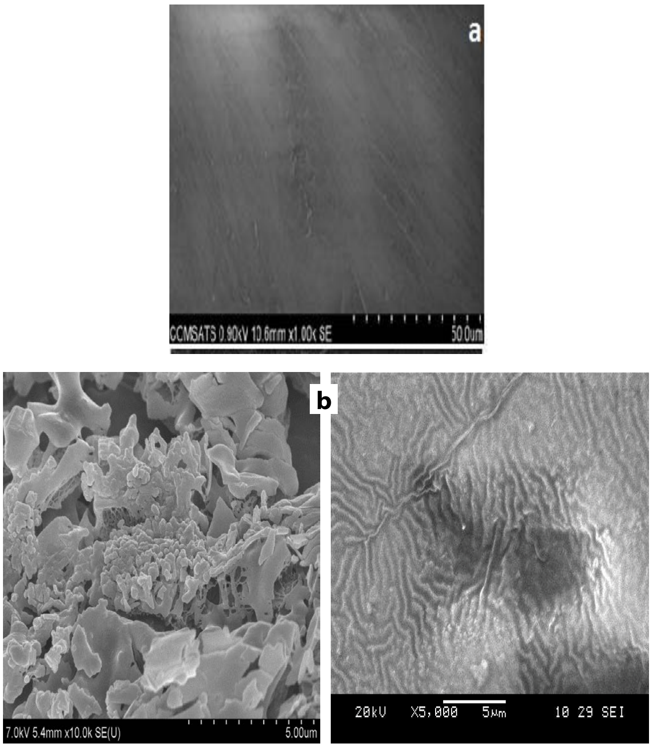

Fig. 2. (a) SEM image of prestine cellulose acetate and (b) SEM image of prepared PIL and CA-PIL membrane.

Table 1
BET surface area analysis of synthesized adsorbents

Properties	PIL	CA-PIL membrane
BET surface area (m^2/g)	171	292
Micropore volume (cm^3/g)	0.05	0.03
Micropore area (m^2/g)	129	53

UV-visible spectroscopy

Most commonly used insecticide “Pirimicarb” was selected for the removal using batch adsorption experiments on prepared adsorbents PIL and CA-PIL membrane. This pesticide is used as insecticide on vegetables and fruits. When wet deposition take place it leaches into the soil and contaminates underground water. Pirimicarb [40,41] was also detected in few crops, indirectly damaging human health. Three variables, that is, time, concentration, and temperature, were studied.

A full scan graph of Pirimicarb was measured using UV-vis spectrophotometer. Wavelength for Pirimicarb was noted at 250 and 316 nm, respectively, as shown in Fig. 4. The percentage removal of Pirimicarb onto prepared PIL was recorded and calculated using absorbance readings (Beer Lambert Law) before and after adsorption process.

Effect of time

Kinetic study plays an important role in the adsorption process [42]. Adsorption of Pirimicarb using synthesized PIL and CA-PIL membrane was carried out under close batch mode of 200 min. First dynamic equilibrium was attained near 30 min followed by adsorption, desorption mechanism also supported by cited literature [43]. It may be attributed to saturation of active sites [7] available on the surface of synthesized adsorbents (PIL and CA-PIL). Maximum removal was achieved using CA-PIL membrane up to 72% as compared with synthesized PIL (55%) as shown in Fig. 5. The repulsion forces between guest molecule on the adsorbent surface and in the solution phase result in decrease in adsorption at later stages. The high rate of adsorption using CA-PIL membrane was due to surface complex mechanism [44] and presence of free acetyl group and hydroxyl groups on polymer backbone [45]. The maximum removal using CA-PIL membrane was also confirmed by the greater surface area of 292 m^2/g as compared with PIL having 171 m^2/g, respectively, as shown in Table 1. Research reported by researchers [46] showed >80% Pirimicarb removal after 6 h with only 2.14 ppm recovery using photo-degradation method.

Effect of concentration

Batch adsorption studies have been conducted by varying concentrations at optimum dose (10 mg). Effect of concentration was studied to check the efficiency of prepared adsorbents for a specific period of time.

Stock solution (10 mg/L) of Pirimicarb was prepared in ethanol using 250 mL volumetric flask. Three working

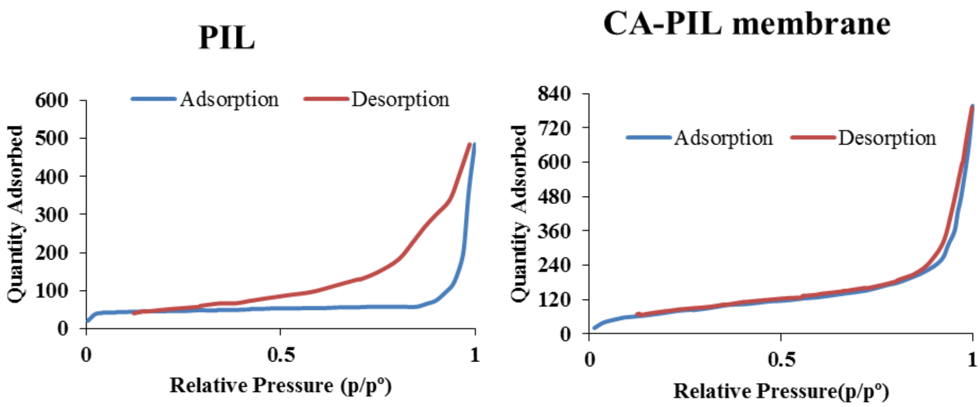

Fig. 3. Nitrogen adsorption isotherms of synthesized PIL and CA-PIL membrane.

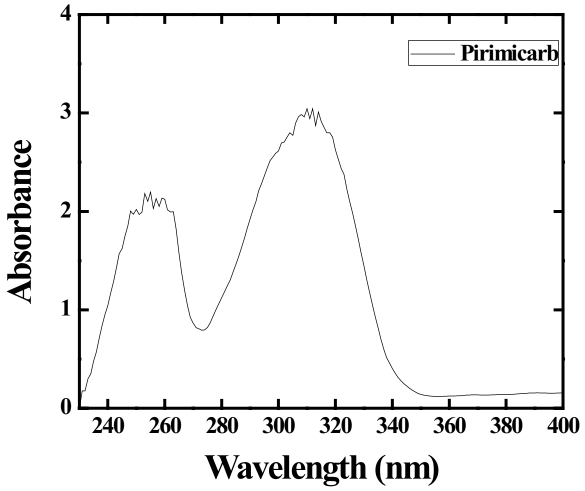

Fig. 4. UV-vis spectrum of Pirimicarb adsorption onto IL.

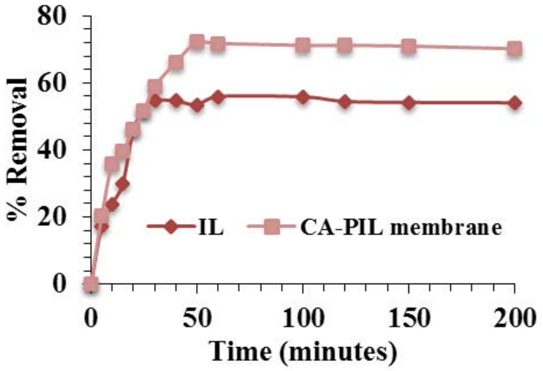

Fig. 5. Percentage removal of Pirimicarb with respect to time.

solutions of 3, 5, and 7 mg/L were separately prepared in a 100 mL beaker to study the effect of varying concentration on adsorption capability of prepared adsorbents (PIL and CA-PIL membrane). Fig. 6 shows that by increasing concentration from 3 to 5 mg/L, adsorption increases and then a decrease trend is observed after increasing concentration up to 7 mg/L. Maximum removal of 64% was observed at 5 mg/L by CA-PIL membrane followed by PIL (50%). Pattern observed can be discussed with reference to availability of many unoccupied sites on adsorbent surface. It can be said that as adsorbate concentration increases, the number of sites available on the adsorbent surfaces is reduced with attainment of saturation point at 5 mg/L (see Fig. 6).

Effect of temperature

The effect of temperature was also studied on prepared PIL and CA-PIL membrane. Temperature was varied from 25°C onward with an interval of 10, 15, 20, and 30, respectively. Fig. 7 shows that as temperature increases from 25°C, adsorption increases until 70°C and then a slight decrease was observed. It may be due to increase in kinetic energy [47]. Similar trend for both prepared adsorbents (PIL and CA-PIL membrane) was observed with maximal removal at 75°C.

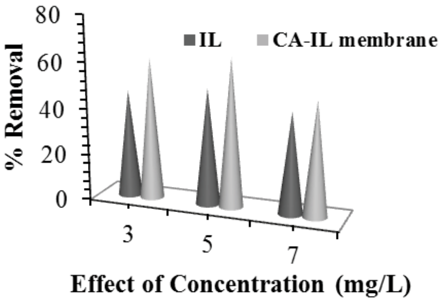

Fig. 6. Percentage removal of Pirimicarb with respect to concentration.

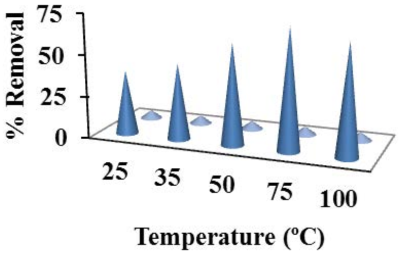

Fig. 7. Percentage removal of Pirimicarb with respect to temperature.

Thermodynamic studies

Different thermodynamic properties, that is, enthalpy (ΔH), entropy (ΔS), and Gibb's free energy change (ΔG), are helpful in providing additional information related to energies during the temperature-dependent sorption [48]. A study was conducted using 5 mg/L adsorbate (Pirimicarb) and 10 mg of adsorbents using following equation:

$$\mathrm{Ln}K_C \; K_C = -\left(\frac{\Delta H}{R}\right)+\left(\frac{\Delta S}{RT}\right) \tag{8}$$

whereas ΔH, ΔS, and T are the enthalpy, entropy, and temperature (K), respectively, R is the general gas constant (8.3143 JK/mol), and K_c is the equilibrium constant.

The plot of ln K_c versus $1/T$ is almost linear throughout temperature range (298–373 K) with regression value of >0.96 for both adsorbents (PIL and CA-PIL membrane). ΔH and ΔS were calculated from linear curve obtained from thermodynamic Eq. (7). The Gibbs free energy (ΔG) is calculated using following equation:

$$\Delta G = \Delta H - T\Delta S \tag{9}$$

Negative ΔG at different temperatures was recorded for both adsorbents (PIL and CA-PIL membrane) as shown in Table 2. This negative sign was attributed to spontaneous nature of sorption [47,49] but ΔH and ΔS positive values were due to endothermic sorption process of pirimicarb onto prepared adsorbents and also indicated that sorption was entropy driven. The low enthalpy and entropy designated toward physisorption mechanism without involving any disruption within chemical bonding of both adsorbents.

Table 2
Different kinetic parameters for sorption studies of Pirimicarb onto prepared PIL and CA-PIL membrane

Sample	Temp. (K)	K_c	ΔG (kJ/mol)	ΔH = Slope × R	ΔS = (Intercept × R)/1,000
PIL	298	19.2	–7.33	22.1	0.035
	308	86.9	–11.4		
	323	43.7	–10.1		
	348	61.9	–11.9		
	373	17.8	–8.93		
CA-PIL membrane	298	19.5	–7.36	12.1	0.005
	308	65.4	–10.7		
	323	43.7	–10.1		
	348	140	–14.3		
	373	27.2	–10.2		

The positive physisorption was corresponding to net gain in degree of freedom of sorbed specie.

The small value of ΔG was also the indication of reversible sorption process and can be more favorable [50] for desorption studies of prepared PIL and CA-PIL membrane. In adsorption process, PIL has played the role of surfactant when get supported by CA and lead to micelles formation. The predicted physiochemical sorption mechanism revealed that in CA-PIL membrane, PIL had formed micellar coating due to hydrogen bonding of the anionic part with the CA surface. Pirimicarb may be adsorbed through multitude interactions involving Π–Π* interactions, electrostatic interactions, and hydrogen bonding [51].

Isotherms and kinetics

Kinetics predicts the adsorption rate and gives important information for designing and modeling the adsorption processes [52]. Fitting supported pseudo-second-order reaction mechanism [53]. The linear plot of t/q_t and t revealed a positive relation and good agreement between calculated and experimental q_e values as compared with pseudo-first-order. Regression coefficient recorded was also close to unity that reflects the physiochemical nature of adsorption process. For intraparticle diffusion model, the three regions in the graph plot Q_t versus $t^{0.5}$ suggested that the sorption portion underwent boundary layer, surface as well as intraparticle diffusion phenomenon. The first linear curve was also attributed toward external and boundary layer effect while second linear curve was defined for diffusion mechanism within pores and third curve was designated to equilibrium constant (K_{id}). The low value of intercept showed lower contribution of the surface sorption in the rate-controlling step as shown in Fig. 8 and Table 3.

Different isothermic models (see Fig. 9) were also applied for fitting experimental results in Eqs. (1)–(7). It can be said that Langmuir, Freundlich, and Temkin equations were seemed to be very good with regression coefficient >0.9 using linear regression analysis [54] as shown in Fig. 10.

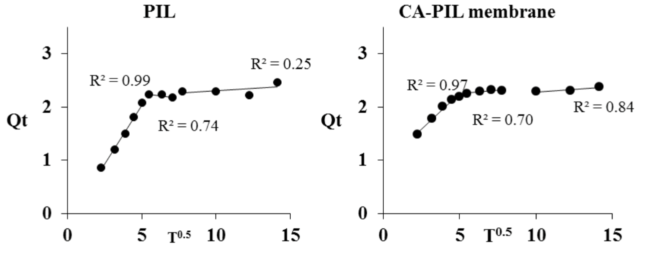

Fig. 8. Intraparticle diffusion model for PIL and CA-PIL membrane.

Table 3
Intraparticle diffusion rate parameter and effective diffusion coefficient

Adsorbents	Phase 1		Phase 2	Phase 3
	K_{id}	C	K_{id}	K_{id}
PIL	0.44	0.16	0.04	0.02
CA-PIL membrane	0.26	0.92	0.02	0.02

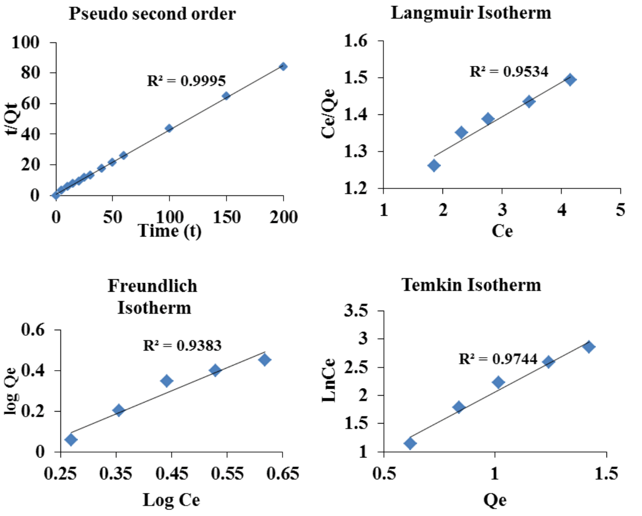

Fig. 9. Adsorption kinetics and isotherms.

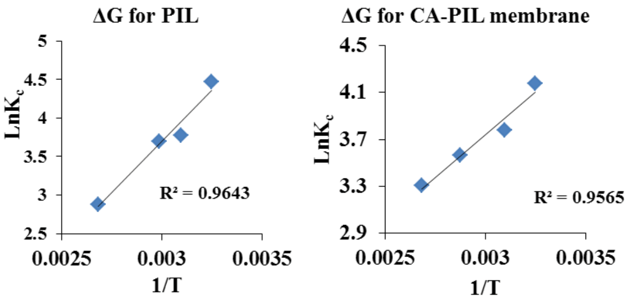

Fig. 10. Gibbs free energy for synthesized PIL and CA-PIL membrane.

5. Conclusion

Present research work was based on synthesis of PILs and membrane using environment-friendly approach. It can be concluded from results that synthesized materials (PIL and CA-PIL membrane) can act as efficient adsorbents for removal of toxic insecticide (Pirimicarb) from wastewater at optimum temperature (70°C) and concentration (5 mg/L). Themaximum percentage removal of 71% was observed using CA-PIL membrane as compared with PIL (55%). Kinetics study favored pseudo-second-order while Langmuir, Temkin, and Freundlich isotherms were the best fit isotherms for the experimental data. The intraparticular diffusion model showed that experimental data were depended on three steps sorption process. Calculation of ΔG, ΔH, and ΔS by thermodynamic studies predicted the reaction as an endothermic physiochemical sorption process.

References

[1] K.M. Somashekar, M. Mahima, K. Manjunath, Contamination of water sources in Mysore City by pesticide residues and plasticizer – a cause of health concern, Aquat. Procedia, 4 (2015) 1181–1188.
[2] M.P.G. de Llasera, M. Bernal-González, Presence of carbamate pesticides in environmental waters from the northwest of Mexico: determination by liquid chromatography, Water Res., 35 (2001) 1933–1940.
[3] P. Christou, T. Capell, Transgenic crops and their applications for sustainable agriculture and food security, Environ. Impact G.M. Crops, (2009) 3–22.
[4] G. Zhang, X. Hu, J. Pan, Spectroscopic studies of the interaction between pirimicarb and calf thymus DNA, Spectrochim. Acta, Part A, 78 (2011) 687–694.
[5] T. Chen, F. Fu, Z. Chen, D. Li, L. Zhang, G. Chen, Study on the photodegradation and microbiological degradation of pirimicarb insecticide by using liquid chromatography coupled with ion-trap mass spectrometry, J. Chromatogr., 1216 (2009) 3217–3222.
[6] M.A. Alawi, L.A. Hasan, K. Tanaka, Improved photocatalytic degradation of insecticide pirimicarb on SiO$_2$ loaded TiO$_2$, Fresenius Environ. Bull., 16 (2007) 403.
[7] B. Gao, J. Wang, F. An, Q. Liu, Molecular imprinted material prepared by novel surface imprinting technique for selective adsorption of pirimicarb, Polymer, 49 (2008) 1230–1238.
[8] A.A.N., EC08, Basic overview of the working principle of a potentiostat/galvanostat (PGSTAT)–electrochemical cell setup, Metrohm Autolab BV, (2011) 1–3.
[9] M. Petkovic, K.R. Seddon, L.P.N. Rebelo, C.S. Pereira, Ionic liquids: a pathway to environmental acceptability, Chem. Soc. Rev., 40 (2011) 1383–1403.
[10] D. Bera, D. Lahiri, A. Nag, Kinetic studies on bleaching of edible oil using charred sawdust as a new adsorbent, J. Food Eng., 65 (2004) 33–36.
[11] S. Wang, Y. Peng, Natural zeolites as effective adsorbents in water and wastewater treatment, Chem. Eng. J., 156 (2010) 11–24.
[12] G.Z. Memon, M. Bhanger, M. Akhtar, F.N. Talpur, J.R. Memon, Adsorption of methyl parathion pesticide from water using watermelon peels as a low cost adsorbent, Chem. Eng. J., 138 (2008) 616–621.
[13] X. Hou, S. Lei, S. Qiu, L. Guo, S. Yi, W. Liu, A multi-residue method for the determination of pesticides in tea using multi-walled carbon nanotubes as a dispersive solid phase extraction absorbent, Food Chem., 153 (2014) 121–129.
[14] X. Zheng, L. He, Y. Duan, X. Jiang, G. Xiang, W. Zhao, S. Zhang, Poly (ionic liquid) immobilized magnetic nanoparticles as new adsorbent for extraction and enrichment of organophosphorus pesticides from tea drinks, J. Chromatogr., 1358 (2014) 39–45.
[15] Q. Zhou, H. Bai, G. Xie, J. Xiao, Trace determination of organophosphorus pesticides in environmental samples by temperature-controlled ionic liquid dispersive liquid-phase microextraction, J. Chromatogr., 1188 (2008) 148–153.
[16] G.A. Olah, T. Mathew, A. Goeppert, B. Török, I. Bucsi, X.-Y. Li, Q. Wang, E.R. Marinez, P. Batamack, R. Aniszfeld, Ionic liquid and solid HF equivalent amine-poly (hydrogen fluoride) complexes effecting efficient environmentally friendly isobutane−isobutylene alkylation, J. Am. Chem. Soc., 127 (2005) 5964–5969.
[17] X. Sun, L H. Uo, S. Dai, Ionic liquids-based extraction: a promising strategy for the advanced nuclear fuel cycle, Chem. Rev., 112 (2011) 2100–2128.
[18] N.V. Plechkova, K.R. Seddon, Applications of ionic liquids in the chemical industry, Chem. Soc. Rev., 37 2008) 123–150.
[19] A. Wilke, J. Yuan, M. Antonietti, J. Weber, Enhanced carbon dioxide adsorption by a mesoporous poly (ionic liquid), ACS Macro Lett., 1 (2012) 1028–1031.
[20] D. Wei-Li, J. Bi, L. Sheng-Lian, L. Xu-Biao, T. Xin-Man, A. Chak-Tong, Functionalized phosphonium-based ionic liquids as efficient catalysts for the synthesis of cyclic carbonate from expoxides and carbon dioxide, Appl. Catal. A, 470 (2014) 18–188.
[21] C.W. Scheeren, V. Hermes, O. Bianchi, P.F. Hertz, S.L. Dias, J. Dupont, Antimicrobial membrane cellulose acetate containing ionic liquid and metal nanoparticles, J. Nanosci. Nanotechnol., 11 (2011) 5114–5122.
[22] F.H.H. Abdellatif, J. Babin, C. Arnal-Herault, L. David, A. Jonquieres, Grafting of cellulose acetate with ionic liquids for biofuel purification by a membrane process: influence of the cation, Carbohydr. Polym., 147 (2016) 313–322.
[23] Q. Yang, J. Wang, W. Zhang, F. Liu, X. Yue, Y. Liu, M. Yang, Z. Li, J. Wang, Interface engineering of metal organic framework on graphene oxide with enhanced adsorption capacity for organophosphorus pesticide, Chem. Eng. J., 313 (2017) 19–26.
[24] A. Derylo-Marczewska, M. Blachnio, A.W. Marczewski, A. Swiatkowski, B. Buczek, Adsorption of chlorophenoxy pesticides on activated carbon with gradually removed external particle layers, Chem. Eng. J., 308 (2017) 408–418.
[25] M. Sharma, S. Hazra, S. Basu, Kinetic and isotherm studies on adsorption of toxic pollutants using porous ZnO@ SiO$_2$ monolith, J. Colloid Interface Sci., 504 (2017) 669–679.
[26] S. Shattar, N. Zakaria, K. Foo, Utilization of montmorillonite as a refining solution for the treatment of ametryn, a second generation of pesticide, J. Environ. Chem. Eng., 5 (2017) 3235–3242.
[27] K. Parveen, U. Rafique, S.Z. Safi, M.A. Ashraf, A novel method for synthesis of functionalized hybrids and their application for wastewater treatment, Desal. Wat. Treat., 57 (2016) 161–170.
[28] W.J. Weber, J.C. Morris, Kinetics of adsorption on carbon from solution, J. Sanit. Eng. Div., 89 (1963) 31–60.
[29] G. Walker, L. Hansen, J.-A. Hanna, S. Allen, Kinetics of a reactive dye adsorption onto dolomitic sorbents, Water Res., 37 (2003) 2081–2089.
[30] C.J. Bradaric, A. Downard, C. Kennedy, A.J. Robertson, Y. Zhou, Industrial preparation of phosphonium ionic liquids, Green Chem., 5 (2003) 143–152.

[31] A.I. Bhatt, I. May, V.A. Volkovich, M.E. Hetherington, B. Lewin, R.C. Thied, N. Ertok, Group 15 quaternary alkyl bistriflimides: ionic liquids with potential application in electropositive metal deposition and as supporting electrolytes, J. Chem. Soc. Dalton Trans., 24 (2002) 4532–4534.

[32] G. Socrates, Infrared and Raman Characteristic Group Frequencies: Tables and Charts, John Wiley & Sons, University of West, London, Middlesex, UK, 2001.

[33] Z. Zhou, X. Zhang, C. Lu, L. Lan, G. Yuan, Polyaniline-decorated cellulose aerogel nanocomposite with strong interfacial adhesion and enhanced photocatalytic activity, RSC Adv., 4 (2014) 8966–8972.

[34] A. Sabir, M. Shafiq, A. Islam, S.M. Khan, T. Jamil, M.T. Zahid, A. Shafeeq, A. Shehzad, A.S. Bhatti, Y. Habib, Influence of polyethylene glycol 600 on cellulose acetate membranes for reverse osmosis desalination, J. Polym. Res., 9 (2015) 291.

[35] A.P. Abbott, T.J. Bell, S. Handa, B. Stoddart, O-Acetylation of cellulose and monosaccharides using a zinc based ionic liquid, Green Chem., 7 (2005) 705–707.

[36] Y. Han, X. Wu, X. Zhang, Z. Zhou, C. Lu, Reductant-free synthesis of silver nanoparticles-doped cellulose microgels for catalyzing and product separation, ACS Sustain. Chem. Eng., 4 (2016) 6322–6331.

[37] Y. Asahi, J. Miura, T. Tsuda, S. Kuwabata, K. Tsunashima, Y. Noiri, T. Sakata, S. Ebisu, M. Hayashi, Simple observation of *Streptococcus mutans* biofilm by scanning electron microscopy using ionic liquids, AMB Express., 5 (2015) 6.

[38] M.P. Singh, Y.L. Verma, A.K. Gupta, R.K. Singh, S. Chandra, Changes in dynamical behavior of ionic liquid in silica nanopores, Ionics, 20 (2014) 507–516.

[39] R. Atkin, N. Borisenko, M. Drüschler, S.Z. El Abedin, F. Endres, R. Hayes, B. Huber, B. Roling, An in situ STM/AFM and impedance spectroscopy study of the extremely pure 1-butyl-1-methylpyrrolidinium tris (pentafluoroethyl) trifluorophosphate/Au (111) interface: potential dependent solvation layers and the herringbone reconstruction, Phys. Chem. Chem. Phys., 13 (2011) 6849–6857.

[40] T. Katagi, Bioconcentration, bioaccumulation, and metabolism of pesticides in aquatic organisms, Rev. Environ. Contam. Toxicol., (2010) 1–132.

[41] A. Widenfalk, J.M. Svensson, W. Goedkoop, Effects of the pesticides captan, deltamethrin, isoproturon, and pirimicarb on the microbial community of a freshwater sediment, Environ. Toxicol. Chem., 23 (2004) 1920–1927.

[42] N. Kannan, M.M. Sundaram, Kinetics and mechanism of removal of methylene blue by adsorption on various carbons – a comparative study, Dyes Pigm., 51 (2001) 25–40.

[43] B. Hameed, J. Salman, A. Ahmad, Adsorption isotherm and kinetic modeling of 2, 4-D pesticide on activated carbon derived from date stones, J. Hazard. Mater., 163 (2009) 121–126.

[44] Y. Tian, M. Wu, R. Liu, Y. Li, D. Wang, J. Tan, R. Wu, Y. Huang, Electrospun membrane of cellulose acetate for heavy metal ion adsorption in water treatment, Carbohydr. Polym., 83 (2011) 743–748.

[45] D. Perera, S. Nataraj, N. Thomson, A. Sepe, S. Hüttner, U. Steiner, H. Qiblawey, E. Sivaniah, Room-temperature development of thin film composite reverse osmosis membranes from cellulose acetate with antibacterial properties, J. Membr. Sci., 453 (2014) 212–220.

[46] M.M. Soliman, Effect of UV-light, temperature, indoor dark and day light storage, on the stability and biological effectiveness of some insecticides, Egypt. Acad. J. Biol. Sci., 3 (2011) 33–42.

[47] M.M. Saeed, M. Ahmed, Effect of temperature on kinetics and adsorption profile of endothermic chemisorption process:–Tm (III)–PAN loaded PUF system, Sep. Sci. Technol., 41 (2006) 705–722.

[48] D. Broznić, Č. Milin, Effects of temperature on sorption-desorption processes of imidacloprid in soils of Croatian coastal regions, J. Environ. Sci. Health., Part B, 47 (2012) 779–794.

[49] S. Rani, D. Sud, Effect of temperature on adsorption-desorption behaviour of triazophos in Indian soils, Plant Soil Environ., 61 (2015) 36–42.

[50] U.A. Qureshi, A.R. Solangi, S.Q. Memon, S.I. Taqvi, N. Memon, Ionic liquid modified resin for the adsorptive removal of dibutyl phthalate: equilibrium, kinetic, and thermodynamic studies, CLEAN – Soil Air Water., 40 (2012) 630–639.

[51] J. Li, Y. Cai, Y. Shi, S. Mou, G. Jiang, Analysis of phthalates via HPLC-UV in environmental water samples after concentration by solid-phase extraction using ionic liquid mixed hemimicelles, Talanta, 74 (2008) 498–504.

[52] M.H. Kalavathy, T. Karthikeyan, S. Rajgopal, L.R. Miranda, Kinetic and isotherm studies of Cu (II) adsorption onto H_3PO_4-activated rubber wood sawdust, J. Colloid Interface Sci., 292 (2005) 354–362.

[53] Y.-S. Ho, G. McKay, Pseudo-second order model for sorption processes, Process Biochem., 34 (1999) 451–465.

[54] E. Ayranci, N. Hoda, Adsorption kinetics and isotherms of pesticides onto activated carbon-cloth, Chemosphere, 60 (2005) 1600–1607.